Chinese Physics C Vol. 40, No. 2 (2016) 027002

Study of a magnetic alloy-loaded cavity for compact synchrotrons*

Hua Shi(施华)[1;1)] Yoshiro Irie(入江吉郎)[2]

[1] Key Laboratory of Particle Acceleration Physics and Technology, Institute of High Energy Physics, Chinese Academy of Sciences, Beijing 100049, China

[2] High Energy Accelerator Research Organization, 1-1 Oho, Tsukuba, Ibaraki 305-0801, Japan

Abstract: Magnetic alloy (MA)-loaded cavities have been widely used in compact proton and heavy-ion synchrotrons, and the MA core is the key issue in their development. Chinese-produced MA has never yet been adopted as core material for an MA-loaded cavity. To use Chinese-produced MA as the core material, it is necessary to study its properties, and compare with MA material produced elsewhere. In this paper, the properties of several MA cores made of Chinese-produced material are measured. Based on the measured results, a schematic design is produced for a cavity which could obtain 1 kV gap voltage with less than 1.5 kW power dissipation in the frequency range of 0.5–7 MHz. The difference between resonant frequencies obtained from simulation and analytical results is less than 10%.

Keywords: magnetic alloy core, coaxial resonant cavity, synchrotron

PACS: 29.20.dk **DOI:** 10.1088/1674-1137/40/2/027002

1 Introduction

Magnetic alloy (MA)-loaded cavities have been widely used in proton and heavy-ion synchrotrons [1–7] due to their wide band of operating frequency, untuned RF system and high accelerating gradient. There are mainly three types of MA core used in RF cavities: Fe-based amorphous metal [1], Co-based amorphous metal [2] and nanocrystalline Fe-based soft magnetic material [3–7]. However, the nanocrystalline Fe-based alloy with the brand name FINEMET, produced by the Hitachi company, is adopted by most accelerators because of its good performance and low cost. In this study, a Chinese-made nanocrystalline Fe-based alloy is examined.

Due to the lack of experience in fabrication of large MA cores, Chinese firms can provide only small-size cores, with an outer diameter of 100 mm. The core property is the key factor for the performance of the RF system, so a platform was established for measuring the properties of MA cores. Several cores with different ribbon materials and different annealing techniques were tested and compared with Hitachi-made cores in Section 2. Based on the measured results, the schematic design of a cavity is described in Section 3, showing that it could obtain 1 kV gap voltage with less than 1.5 kW power dissipation in the frequency range of 0.5–7 MHz. The analytical and simulation results are then compared for this cavity design. Some conclusions are then given in Section 4.

2 Magnetic alloy cores

Compared with soft ferrite material, the advantages of the MA-loaded RF cavities are summarized as follows.

1) Wide band operating frequency: the initial permeability of MA is very high, and the μ_s' (the real part of complex permeability) decreases with frequency, so μ_s' is enough to satisfy the very wide band frequency.

2) High and stable shunt impedance: the parallel complex permeability (suffix p) is adopted to estimate the shunt impedance [8]

$$R_{\rm ma}=n\mu_0 t\ln\left(\frac{r_{\rm o}}{r_{\rm i}}\right)\left(\mu_{\rm p}'Q_{\rm ma}f\right), \qquad (1)$$

where t, $r_{\rm o}$ and $r_{\rm i}$ are the thickness, the outer and inner radii of the MA cores, respectively, μ_0 is the vacuum permeability, n is the number of MA cores, and $\mu_{\rm p}'Q_{\rm ma}f$ is the impedance product, which is independent of size of core. The $\mu_{\rm p}'Q_{\rm ma}f$-product of an MA core is high, greater than 2×10^9 Hz, so the impedance of an MA-loaded cavity can become high enough. Also, the $\mu_{\rm p}'$ and $Q_{\rm ma}$ properties of the MA material are stable under varying RF magnetic field density ($B_{\rm rf}$) and temperature.

3) Bias current source is not required and this makes the RF system simple: because the MA cores have a low-Q value of ∼0.5 and high impedance, they are well suited

Received 13 April 2015, Revised 10 September 2015

∗ Supported by National Natural Science Foundation of China (11175194)

1) E-mail: shih@ihep.ac.cn

to a tuning-free wide band cavity and it is unnecessary to have a bias current tuning system. The complicated bias winding in the cavity is dispensable and the whole RF system becomes simple and compact.

Two Chinese firms, Tiantong and Liyuan, developed several small MA cores with the specifications listed in Table 1. The names of the three kinds of cores in the first column are given according to the name of the materials in the fifth column. 1k107-1 was made by Tiantong, while 1k107-2 and FT-3 were made by Liyuan. In the fifth column, 1k107 is Chinese-produced 1k107 25 μm-thickness ribbon, and FT-3 is Hitachi FT-3 18 μm-thickness ribbon. The sixth column refers to whether or not a magnetic field $H_{\rm v}$ is applied vertically during annealing. We measured the magnetic properties of these cores with Network Analyzer (Agilent 4395A). Before the measurement, a calibration was made with different conditions. One MA core was wound with a short single-turn loop coil, and the impedance as a function of frequency from 0.5 to 20 MHz could be measured. Based on the measurement results, the $\mu_{\rm s}'$, the imaginary part of complex permeability $\mu_{\rm s}''$, $Q_{\rm ma}$ and other parameters can be calculated.

Table 1. Specifications of the Chinese MA cores.

name	$2r_{\rm o}$/mm	$2r_{\rm i}$/mm	t/mm	material	annealing
1k107-1	100	50	25	1k107 (25 μm)	
1k107-2	130	60	25	1k107 (25 μm)	$H_{\rm v}$
FT-3	130	60	25	FT-3 (18 μm)	$H_{\rm v}$

Figure 1 shows the frequency variation with permeability of 1k107-1 and 1k107-2 in the 0.5–20 MHz frequency band. The ribbons of the two cores are the same, but 1k107-2 was annealed with a vertical magnetic field, which can increase the complex permeability by a factor of 2–3.

Compared with the Hitachi cores, the 1k107-1 properties are similar to those of the FT3M-1 core, as shown in Fig. 2. The FT3M-1 core was developed by Hitachi for the JHF project [9] in the late 1990s. After improving the manufacturing technology, the $\mu_{\rm p}'Q_{\rm ma}f$-product of the new Hitachi FT3M-2 cores (-■-) for the J-PARC project [10] is about 40% higher than that of the 1k107-1 (-▲-), as shown in Fig. 3. Fig. 3 also shows the 1k107-2 (-▼-) and FT-3 (-♦-), and we can see that properties of these two cores are similar to the Hitachi FT3L cores (-□-), which were developed recently [10] with 13 μm-thickness ribbon and applying $H_{\rm v}$ during annealing. For fabricating cores with an outer diameter of 500 mm, winding, annealing, coating and other fabrication procedures must be very well controlled, however, the magnetic properties of the cores cannot meet the requirements.

In conclusion, for small MA cores, the ribbons and manufacturing processes of the 1k107-1 and 1k107-2 are similar to the Hitachi material. Because very few

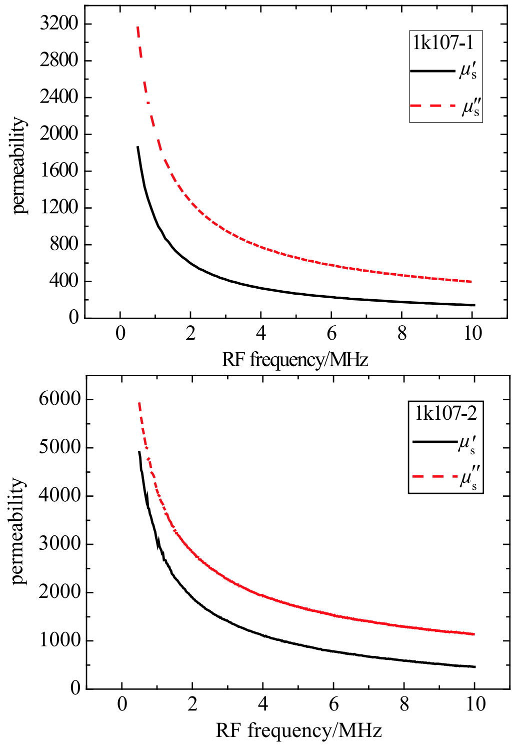

Fig. 1. (color online) Permeability versus frequency for 1k107-1 and 1k107-2.

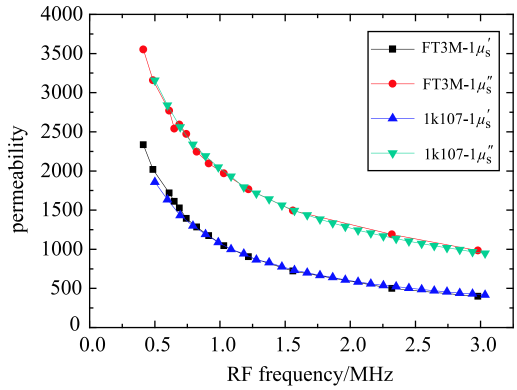

Fig. 2. (color online) Permeability comparison between 1k107-1 and FT3M-1.

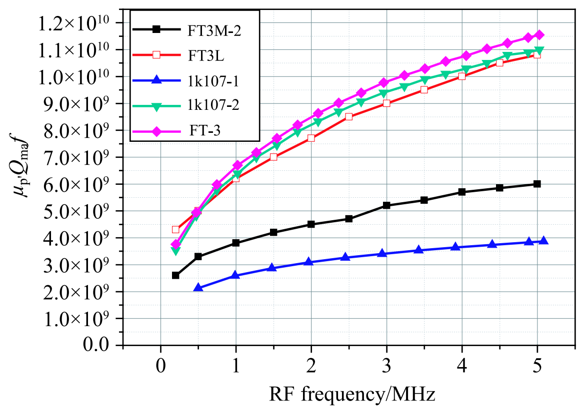

Fig. 3. (color online) $\mu_{\rm p}'Q_{\rm ma}f$-product comparison.

Chinese firms have an annealing oven with a vertical magnetic field for large cores, the design of the RF cavity is based on the measurement data of the 1k107-1.

3 RF cavity

3.1 Design of the RF cavity

A coaxial resonator loaded with several MA cores is adopted in the design, which can be characterized as an LC lumped cavity. Figure 4(a) shows the equivalent circuit, where U_g is the gap voltage, C is the equivalent capacitance of the accelerating gap, L_s is the total inductance including the loaded MA cores and the empty cavity inductance, and R_s is a resistance which represents the total power loss in the MA cores.

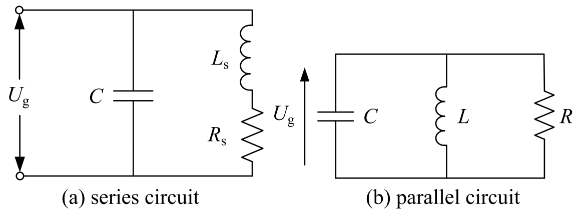

Fig. 4. Equivalent circuit of MA-loaded coaxial resonator.

C is given [11] by

$$C=\varepsilon_0\varepsilon_r\frac{\pi\left(r_{\rm gapo}^2-r_{\rm gapi}^2\right)}{d_{\rm gap}}, \tag{2}$$

where ε_0 is the vacuum permittivity, ε_r is the ceramic gap permittivity, and $d_{\rm gap}$, $r_{\rm gapo}$, and $r_{\rm gapi}$ are the gap length and the radii of the outer and inner ceramic gaps, respectively. L_s is calculated by

$$\begin{aligned}L_s&=L_{\rm ma}+L_c\\&=n\frac{\mu_0}{2\pi}\mu_s' t\ln\frac{r_o}{r_i}+\frac{\mu_0}{2\pi}\left(l_{\rm cav}\ln\frac{r_{\rm cav}}{r_{\rm duct}}-nt\ln\frac{r_o}{r_i}\right),\end{aligned} \tag{3}$$

where $L_{\rm ma}$ is the inductance of the loaded MA cores, L_c is that of the empty cavity, and $l_{\rm cav}$, $r_{\rm cav}$ and $r_{\rm duct}$ are the cavity length and the radii of the outer and inner conductors of the cavity, respectively. R_s is calculated by

$$R_s=nf\mu_0\mu_s'' t\ln\frac{r_o}{r_i}. \tag{4}$$

By transforming the series circuit into an RLC parallel circuit (Fig. 4(b)), the parameters L and R are obtained as

$$2\pi fL=\frac{R_s^2+(2\pi fL_s)^2}{2\pi fL_s}, \tag{5}$$

$$R=\frac{R_s^2+(2\pi fL_s)^2}{R_s}. \tag{6}$$

The resonant frequency f_r and Q-value are given by

$$2\pi f_r=\frac{1}{\sqrt{LC}}, \tag{7}$$

$$Q=\frac{1}{2\pi f_r}\frac{R}{L}. \tag{8}$$

The cavity power loss is given by

$$P=\frac{U_g^2}{2R}. \tag{9}$$

The cavity impedance is obtained [12] as

$$Z=\frac{1}{\sqrt{\dfrac{1}{R^2}+\left(\omega C-\dfrac{1}{\omega L}\right)^2}}, \tag{10}$$

where angular frequency $\omega=2\pi f$.

Based on the relevant RF machine parameters [13] (shown in Table 2), a schematic diagram of the MA-loaded cavity is shown in Fig. 5, and the design specifications [13] are summarized in Table 3. The RF cavity is a single gap structure which consists of two coaxial resonators loaded with MA cores. The length and diameters of the inner and outer conductors of the cavity are 550, 150 and 550 mm respectively. The outer conductor could be fabricated from a metal-mesh plate to cool the MA cores by air cooling. The length of the accelerating gap is 50 mm. The number of MA cores is 8 and the core has an inner diameter of 260 mm, outer diameter of 500 mm and thickness of 25 mm. The cavity impedance is designed as (490±185) Ω in the operating frequency range of 0.5–7 MHz.

Table 2. Relevant RF machine parameters [13].

circumference/m	33.6
injection energy/MeV	10
max. extraction energy/MeV	300
repetition rate/Hz	0.5
accumulated number of particles	5×10^9

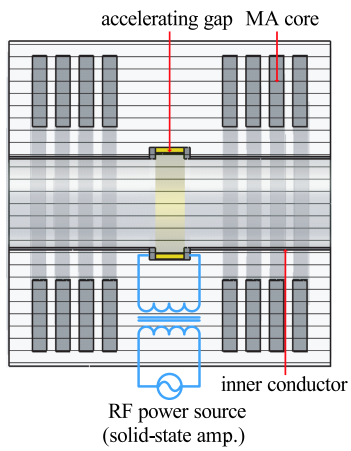

Fig. 5. (color online) Schematic diagram of the MA-loaded accelerating cavity.

Table 3. Design specifications of the RF cavity.

operation frequency	0.5–7 MHz
gap voltage	1 kV
cavity impedance	(490±185) Ω((60±25) Ω/core)
cavity structure	coaxial resonator × 2
	cavity length: 550 mm
	outer conductor diameter: 550 mm
	inner conductor diameter: 150 mm
accelerating gap	gap length: 50 mm
	number of gaps: 1
core material	1k107-1
core shape	toroid
	outer diameter: 500 mm
	inner diameter: 260 mm
	thickness: 25 mm
number of cores	8
cavity power loss	< 1.5 kW
	<200 W/core
core cooling	forced air-cooling
power feeding	1:10 impedance transformer coupling

A solid-state (transistor) amplifier is employed as an RF power source. Impedance matching between the cavity, feeding line and the power source is indispensable to produce a high voltage at the accelerating gap. The impedances of the power source and the feeding line are 50 Ω, and a 1 : 10 impedance transformer will be used to match the feeding line and cavity.

Table 4 lists the design parameters for the equivalent circuit (Fig. 4(b)) at the frequencies of 0.5, 1, 3, 5 and 7 MHz. The complex permeabilities used for the MA cores are the test data of the 1k107-1 at these frequencies. The shunt impedance R and the inductance L of the cavity are calculated by Eqs. (3–6). The equivalent capacitance of the accelerating gap C is calculated by Eq. (2). We determine the size and number of MA cores so that the resonant frequency lies in the range 0.5–7 MHz. At 1 kV operating voltage, the total power dissipation of MA cores is less than 1.5 kW (<200 W/core). According to Hitachi operating experience [14], forced air-cooling is enough to cool the MA-loaded cavity.

Table 4. Design parameters of the equivalent circuit representing the RF cavity.

f/MHz	0.5	1	3	5	7
(μ_s', μ_s'')	(1857, 3159)	(1000, 1931)	(418, 947)	(268, 663)	(200, 514)
R/Ω	349.75	403.13	559.88	636.91	685.54
L/μH	188.85	123.38	66.65	49.37	39.18
C/pF			20		
Z/Ω	304.18	364.95	545.12	636.88	671.44
f_r/MHz	2.59	3.20	4.36	5.06	5.68
P/kW	1.43	1.24	0.89	0.79	0.73

3.2 Simulation of RF cavity

CST Microwave Studio [15] is used to simulate the cavity. Fig. 6 shows the electromagnetic field distribution of the cavity at 5.42 MHz (the complex permeability of the MA cores is (268, 663)@5 MHz). As shown in Fig. 6(a), the electric field is concentrated at the accelerating gap, which satisfies the RF cavity design. From Fig. 6(b), we can see that the magnetic field is distributed almost uniformly in the two coaxial resonators. The main source of power dissipation in the RF cavity is magnetic loss of MA cores.

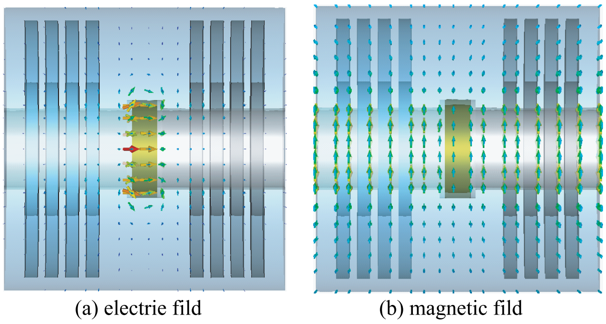

Fig. 6. (color online) Electromagnetic field distribution of accelerating cavity.

We use the impedance relative permeability μ_z [16] to compare the analytical and CST simulation results, with

$$\mu_z = \sqrt{\mu_s'^2 + \mu_s''^2}. \tag{11}$$

Figure 7 shows the μ_z dependence of analytical and simulation resonant frequencies, and we can see that the two values agree well.

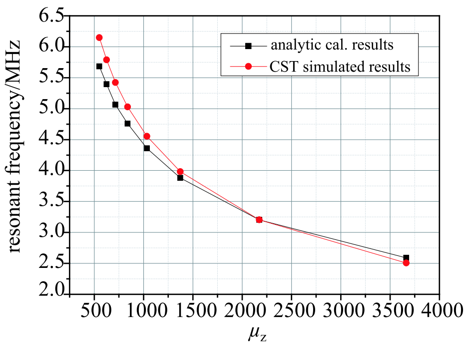

Fig. 7. (color online) Analytical and simulation resonant frequencies versus μ_z.

The results of CST simulation are shown in Table 5, in which f_{cst} and Q_{cst}, the deviationf_{rdev} between f_r and f_{cst}, and Q_{dev} between Q_{ma} and Q_{cst} are given. The difference of Q-value is 50%–90%.

We also compare the analytical and simulated shunt impedance at resonant frequency Z_r and Z_{cst} in Table 6. Z_r equals R_r at resonant frequency f_r, and is rewritten as

$$Z_r = R_r = \frac{R_{sr}^2 + (2\pi f_r L_s)^2}{R_{sr}}, \tag{6'}$$

where R_{sr} is the series resistance at f_r

$$R_{sr} = n f_r \mu_0 \mu_s'' t \ln \frac{r_o}{r_i}. \qquad (4')$$

Z_{cst} is estimated at f_{cst} and calculated by

$$Z_{cst} = \frac{Q_{cst}}{(2\pi f_{cst})C}. \qquad (12)$$

The deviation Z_{dev} between Z_r and Z_{cst} is 50%–70%.

Table 5. Analytical and CST simulation results of cavity.

f/MHz	0.5	1	3	5	7
(μ_s', μ_s'')	(1857, 3159)	(1000, 1931)	(418, 947)	(268, 663)	(200, 514)
μ_z	3664	2174	1035	715	552
f_r/MHz	2.59	3.20	4.36	5.06	5.68
f_{cst}/MHz	2.51	3.20	4.55	5.42	6.15
f_{rdev}/%	3.08	0	4.36	7.11	8.27
Q_{ma}	0.588	0.517	0.441	0.404	0.389
Q_{cst}	0.875	0.823	0.770	0.745	0.736
Q_{dev}/(%)	48.7	59.0	74.6	84.5	89.0

We think the main reason for these differences is due to the limitations of CST in simulating cavities loaded with high-loss magnetic material. This is the same result as that obtained in our previous study [17]. In Ref. [17], it is shown that the analytical results for the cavity impedance agree well with the measurements for the MA-loaded testing cavity where the cavity Q-value is ∼0.6 [14]. Ref. [17] also shows that the analytical and simulation results for resonant frequencies and Q-values agree very well for $Q > 2$, but not well for $Q < 2$.

Table 6. Analytical and CST simulation shunt impedance of cavity.

f_r/MHz	2.59	3.20	4.36	5.06	5.68
Z_r/Ω	1810	1291	813	645	556
f_{cst}/MHz	2.51	3.20	4.55	5.42	6.15
Z_{cst}/Ω	2774	2043	1344	1092	951
Z_{dev}/%	53.2	58.3	65.3	69.4	70.9

4 Conclusions

The properties of small-size MA cores made by Chinese firms have been measured and compared with those of Hitachi-made cores. Based on the measured results, an RF cavity for proton and heavy-ion synchrotrons has been designed. The considered frequency range is from 0.5 to 7 MHz. The cavity shunt impedance reaches (490±185) Ω, and the total power dissipation with 1kV accelerating voltage is less than 1.5 kW, so forced air-cooling can meet the cooling requirements. Further investigation is required for manufacturing full size (outer diameter about 500 mm) cores with similar properties.

The electromagnetic field distributions with CST simulation are very useful for checking the cavity design. The difference between simulation and analytical resonant frequencies is less than 10%. However, for Q-factor and cavity impedance, there are some differences between the analytical and simulation results, which needs further investigation.

References

1 M. Bohnke, F. J. Etzkorn, R. Maier et al, Broadband Synchrotron Cavity for COSY with Minimum Size Based on VitroPerm, in *Proceedings of PAC1999* (New York, USA, 1999), p. 851

2 M. Kanazawa, T. Misu, A. Sugiura et al, Nucl. Instrum. Methods. A, **566**(2): 195 (2002)

3 M. Fujieda, Y. Iwashita, A. Noda et al. Phys. Rev. ST Accel. Beams, **2**: 122001 (1999)

4 G. Hutter, P. Hulsmann, and W. Vinzenz, The Bunch Compressor System for SIS18 at GSI, in *Proceedings of EPAC2004* (Switzerland, 2004), p. 1165

5 M. Muto, S. Ninomiya, and M. Toda, Non-resonant Accelerating System at the KEK-PS Booster, in *Proceedings of EPAC2004* (Switzerland, 2004), p. 1027

6 R. Garoby, M. Haase, P. Maesen et al, The LEIR RF System, in *Proceedings of PAC2005* (Knoxville, Tennessee, USA, 2005), p. 1619

7 F. Noda, F. Ebina, H. Nishiuchi et al, Conceptual Design of Carbon/proton Synchrotron for Particle Beam Therapy, in *Proceedings of PAC2009* (Vancouver, British Columbia, Canada, 2009), p. 1300

8 H. Nakayama, E. Ezura, M. Fujieda et al, A Measurement System using GP-IB for a Magnetic Core Test Cavity, in *Proceedings of APAC1998* (Tsukuba, Japan, 1998), p. 393

9 M. Fujieda, Y. Mori, H. Nakayama et al, Studies of Magnetic Cores for JHF Synchrotrons, in *Proceedings of PAC1997* (Vancouver, British Columbia, Canada, 1997), p. 2992

10 C. Ohmori, O. Araoka, E. Ezura et al, High Gradient Magnetic Alloy Cavities for J-PARC Upgrade, in *Proceedings Of IPAC2011* (Kursaal, San Sebastian, Spain, 2011), p. 2885

11 C. F. Xie and K. J. Rao, *Electromagnetic Fields and Waves* Second edition (Beijing: Higher Education Press, 1998), p. 64 (in Chinese)

12 P. Z. Ning and D. F. Min, *Microwave Transmission Technology* (Shanghai: Shanghai Scientific and Technical Publishers, 1985), p. 232 (in Chinese)

13 S. N. Fu et al, (Institute of High Energy Physics, CAS), *The Design Report of Proton Synchrotron for Harbin Institute of Technology*, 2012

14 K. Saito and J. I. Hirota, F. Noda, Nucl. Instrum. Methods. A, **402**(1): 1 (1998)

15 http://www.cst.com

16 http://www.hitachi-metals.co.jp/e/products/elec/tel/pdf/hl-fm9-g.pdf, retrieved 5th January 2015

17 H. Shi and Y. Irie, *Simulation of Magnetic Core-loaded Coaxial cavity*, Internal report, 2014